Fear and safety learning differentially affect synapse size and dendritic translation in the lateral amygdala

Linnaea E. Ostroff[a,1], Christopher K. Cain[a], Joseph Bedont[a,b], Marie H. Monfils[a], and Joseph E. LeDoux[a,c]

[a]Center for Neural Science, New York University, New York, NY 10003; [b]Department of Neuroscience, Johns Hopkins University School of Medicine, Baltimore, MD 21205; and [c]Emotional Brain Institute, Nathan S. Kline Institute for Psychiatry Research, Orangeburg, NY 10962

Fear learning is associated with changes in synapse strength in the lateral amygdala (LA). To examine changes in LA dendritic spine structure with learning, we used serial electron microscopy to reconstruct dendrites after either fear or safety conditioning. The spine apparatus, a smooth endoplasmic reticulum (sER) specialization found in very large spines, appeared more frequently after fear conditioning. Fear conditioning was associated with larger synapses on spines that did not contain a spine apparatus, whereas safety conditioning resulted in smaller synapses on these spines. Synapses on spines with a spine apparatus were smaller after safety conditioning but unchanged with fear conditioning, suggesting a ceiling effect. There were more polyribosomes and multivesicular bodies throughout the dendrites from fear conditioned rats, indicating increases in both protein synthesis and degradation. Polyribosomes were associated with the spine apparatus under both training conditions. We conclude that LA synapse size changes bidirectionally with learning and that the spine apparatus has a central role in regulating synapse size and local translation.

dendritic spine | fear conditioning | polyribosome | spine apparatus | lateral amygdala

The lateral amygdala (LA) fear circuit provides a unique model for investigating the synaptic basis of memory. The LA is critical for the acquisition and storage of auditory fear conditioning, a robust behavioral paradigm in which animals learn to associate a previously neutral tone with an aversive stimulus, such as a footshock (1, 2). In conditioned inhibition, tones and shocks are arranged such that the tone predicts the absence of the shock; the tone thus becomes associated with safety and suppresses fear (3). Tone-evoked physiological responses in the LA are strengthened with fear conditioning and weakened with conditioned inhibition, suggesting that LA synapse strength encodes the fear response to the tone (1, 2, 4–6).

Auditory inputs to LA cells form synapses on dendritic spines, tiny compartments that may allow local regulation of synaptic transmission and structure (7–12). Experimentally-induced changes in synaptic strength such as long-term potentiation (LTP) and depression (LTD) alter spine size in immature hippocampus in vitro, with LTP generally associated with larger spines and LTD with smaller spines (13–16). Although LTP and LTD are considered models of learning, it is unknown whether spine structure is affected by associative learning in the adult animal. To address this question, we took advantage of the known effects of fear learning on LA synaptic strength and used serial section transmission electron microscopy (ssTEM) to reconstruct spiny dendrites from adult rat LA after either fear conditioning or conditioned inhibition training.

Enlarged spines have been proposed as a locus for information storage, with smaller spines representing memory capacity (10, 17). Very large spines typically contain a spine apparatus, a membranous organelle that has been reported to be involved in learning and synaptic plasticity (18). We found that the effects of learning on synapse size differed depending on the presence of the spine apparatus. Protein synthesis is necessary for LA LTP and for consolidation of fear conditioning (19–21). Dendritic translation is

clearly involved in hippocampal LTP and is suspected to occur with fear conditioning, although this has not been directly observed (22–25). We found that there were more polyribosomes in LA dendrites after fear conditioning and that their presence in spines was differentially associated with changes in synapse size.

Results

Behavioral Evidence for Single-Session Fear or Safety Learning. To compare spine morphology in adult rats during consolidation of fear learning, we designed and tested two training protocols of equal length with equal numbers of tone and shock presentations. In the fear conditioning (FC) protocol each tone coterminated with a footshock, whereas in the conditioned inhibition (CI) protocol footshocks were interleaved with tones in an explicitly unpaired manner (Fig. 1A).

A third, naïve group of rats was subjected to identical handling and exposure to the conditioning box but received no tones or shocks. One day after training, only the FC rats display freezing to the tone (Fig. 1B). We then used two standard tests, summation and retardation of acquisition, to establish that the CI procedure produces long-term behavioral inhibition to the unpaired tone (3). Summation tests demonstrate that the tone can suppress freezing elicited by other fearful stimuli. For the context summation test, animals were given either CI training or control training in which the first four tones were omitted. One day later, animals were returned to the shock context and freezing was assessed for 30-s periods before, during, and after tone presentations. CI animals showed significant suppression of context freezing during the tone, whereas control animals did not (Fig. 1C). Rats subjected to our CI protocol also passed a cue summation test, which shows that the tone is capable of suppressing fear of a conditioned stimulus that was not present during the CI training session (Fig. S1). The retardation test demonstrates that the CI tone excites fear less readily when subsequently paired with shock. One day after CI training, rats were given two pairings of the tone with shock in a novel context. Control rats did not receive CI training. When tested the next day, CI rats showed less freezing to the tone than did control rats (Fig. 1D).

The Spine Apparatus Is Associated with Large Synapses and Appears After Learning. For ssTEM experiments, animals were subjected to either the FC or CI procedure or control handling (the naïve group). One hour after the first shock in each training protocol, animals were perfused with mixed aldehydes and the left LA was processed for ssTEM. Although we could not test long-term memory in rats used for ssTEM, learning was evident during the

Fig. 1. Behavior and spine numbers. (*A*) Training protocols for fear conditioning (*Upper*) and conditioned inhibition (*Lower*) indicating the exact timing of tones (black bars) and footshocks (lightning bolts). (*B*) One day after training, the fear conditioning protocol produces freezing to the tone. (*C*) The tone suppresses fear of the context in conditioned inhibition (CI) trained but not control rats (*n* = 8 per group). (*D*) CI trained rats subsequently acquire less fear to the tone than do control rats (*n* = 8 per group). (*E*) Lateral amygdala (LA) section embedded in resin for section transmission electron microscopy showing approximate area of tissue collected for analysis (asterisk). (*F*) EM of LA neuropil showing a dendrite with a spine carrying a PSD apposed to an axon with docked vesicles. All graphs show means ± SEM (*P < 0.01).

training session and the ssTEM rats displayed similar acquisition as the rats used for memory tests (Fig. S1). Auditory brain areas send heavy projections to the dorsal tip of the LA, whereas multimodal sensory and higher cognitive areas project to ventral LA and the basal amygdaloid nucleus (7, 8, 26, 27). Because we were interested in the effects of different auditory associations as opposed to context learning, we sampled tissue from the dorsal tip of the LA just under the dense fiber bundles (Fig. 1*E*). Digitized serial electron micrographs from this area were aligned and spiny dendrites were reconstructed in 3D. Spines are easily identified in ssTEM as dendritic protrusions bearing a postsynaptic density (PSD) in apposition to an axonal bouton containing synaptic vesicles (Fig. 1*F*). Each spine's complete PSD area was measured in 2D and its head volume was measured in three dimensions.

Smooth endoplasmic reticulum (sER) is visible throughout the dendrites, where it forms a generally continuous network and

sometimes extends into spines (Fig. 2*A*). In some spines, the sER forms a spine apparatus, a specialized organelle composed of membranous cisterns interleaved with dense-staining plates (28) (Fig. 2 *A* and *B*). Approximately 20% of LA spines in our dataset contained a spine apparatus, similar to the numbers found in adult hippocampus (29, 30). In another 10% of LA spines, sER from the dendrite extended into the spine but did not form a proper spine apparatus. We categorized each spine for analysis according to its association with the sER network as follows: sER-free (no connection to the sER), SA (containing a spine apparatus), and sER (containing sER but no spine apparatus). In the naïve training group SA spines had larger PSDs and larger head volume than other spines, and sER spines had larger PSD area than sER-free spines (Fig. 2 *C* and *D*). Spine surface area was also larger on SA spines (Fig. S2).

To determine whether larger synapses had larger spine apparatuses, we measured the surface area of the spine apparatus membrane, which did indeed correlate with PSD area (Fig. 2*E*). The number of spine apparatus dense plates ranged from two to six and was also correlated with the size of the PSD ($r^2 = 0.27$, $P < 0.001$), as in hippocampus (29). In approximately 60% of sER spines, the sER extended into the spine head (in the other 40% of spines the sER simply entered the spine neck). Purkinje cell spines, which all lack a spine apparatus, contain sER in proportion to PSD area (31). We measured the surface area of the sER inside sER spine heads to see whether it had a similar relationship to the PSD; it did not (Fig. 2*F*). The spine apparatus itself, as opposed to a simple extension of the sER from the dendrite, thus tracks the synapse morphologically in the LA.

We compared the frequency of each spine type along the dendrites among training groups, to see whether there was an effect on absolute spine numbers. In naïve animals the frequencies of the three spine types were uncorrelated (Fig. S3). There were more SA spines with FC training, but sER-free and sER spine numbers were stable. Filopodia, protrusions without synapses, were also stable across training groups at about 7% of all protrusions (Fig. 2*G*). The distribution of spine type frequencies did not change between the groups (Fig. S4).

Synapse Size Changes Bidirectionally with Learning. Both PSD area and synapse strength have been shown to increase with spine head volume in the hippocampus (10, 32, 33). Our measurements confirm that head volume and PSD area were positively correlated in the LA in all three training groups (FC: $r^2 = 0.84$, $P < 0.001$; naïve: $r^2 = 0.79$, $P < 0.001$; CI: $r^2 = 0.92$, $P < 0.001$). Because FC and CI training produce bidirectional changes in synapse strength, we expected synapse size to reflect learning as well. As predicted, PSD area on sER-free spines increased with FC and decreased with CI (Fig. 3 *A* and *B*). The head volume of these spines decreased with CI and, curiously, also with FC (Fig. 3*C*). Although the effect of FC could be due to spine shrinkage, it could also reflect a transition of larger spines into sER or SA spines, leaving only smaller spines in the sER-free population. In contrast to sER-free spines, FC did not affect synapse size or head volume on SA spines, although both decreased with CI (Fig. 3 *D* and *F*). There were no changes in sER spines with learning (Fig. 3 *G–I*). This is curious considering that these spines resemble sER-free spines in size but would be explained if this group were transitional and transient, representing spines in the process of either building or removing a spine apparatus. The distribution of PSD areas on the three spine type frequencies was not different after training (Fig. S4), suggesting that synapses across the range of sizes are susceptible to bidirectional plasticity. Spine surface area decreased with CI for sER-free and SA spines but was unchanged for sER spines (Fig. S2). Besides spine synapses, we also measured symmetric and asymmetric synapses on dendritic shafts and found that asymmetric synapses shrink with CI (Fig. S5).

Fig. 2. Smooth endoplasmic reticulum (sER) and the spine apparatus. (*A*) Reconstructed dendrite showing post-synaptic densities (PSDs) (red), sER (yellow), and the spine apparatus (orange). Gray cube = 1 μm³. (*B*) EM of spine head containing a spine apparatus (arrow). (*C*) PSDs on SA spines (spines that contain a spine apparatus) are larger than both sER-free and sER spine PSDs, and sER spine PSDs are larger than sER-free spine PSDs (*$P < 0.0005$). (*D*) SA spines have greater head volume than sER-free or sER spines (*$P < 0.0005$). (*E*) SA surface area is correlated with PSD area ($r^2 = 0.55$, $P < 0.01$). (*F*) PSD area is not correlated with sER area in spines where sER enters the spine head ($r^2 = 0.0077$, $P = 0.70$). (*G*) Spine density is stable with training, except for an increase in SA spines with fear conditioning (FC) (*$P < 0.05$). Bar graphs show means ± SEM.

Polyribosomes Increase with Fear Conditioning. Sites of protein synthesis are visible in the EM as polyribosome clusters, which are routinely observed in hippocampal dendrites (34–36). Polyribosomes were identified as clusters of at least three black puncta (15–25 nm in diameter) and classified as being in the dendritic shaft or in a spine, with spine polyribosomes further classified as being in the spine head or in the base or neck (Fig. 4 *A* and *B*). The base was defined as the area within 150 nm of the neck origin. The overall frequency of polyribosomes in both the dendritic shafts and spines increased in the FC group (Fig. 4*C*). The increase in spine polyribosomes with FC was not due to an increase in the number per spine, which averaged 1.5 ± 0.1, 2.0 ± 0.1, and 1.8 ± 0.2 for sER-free, SA, and sER spines, respectively, and did not change with FC. Instead, polyribosomes appeared in

more spines, specifically in the heads of SA spines and the bases and necks of sER-free spines (Fig. 4*D*).

We examined the effect of training on spine size with respect to polyribosomes, because they are associated with synapse growth in hippocampal LTP (35, 36). PSD area on sER-free spines was larger with polyribosomes in all groups, and there was no interaction between training and polyribosomes (Fig. 4*E*). On SA spines, PSD area was larger with polyribosomes for the FC and naïve groups only, and was decreased on CI spines with polyribosomes relative to the naïve group (Fig. 4*F*). There was no effect of polyribosomes on PSD area on sER spines (Fig. 4*G*).

In all three training groups, spine and shaft polyribosome frequency were positively correlated (Fig. 5*A*). This indicates that polyribosomes are not being redistributed between spines and dendrites,

Fig. 3. Effects of training on spine size. (*A*) Reconstruction of a smooth endoplasmic reticulum (sER)-free spine (colors as in Fig. 2*A*). (*B*) Postsynaptic density (PSD) area of sER-free spines changes bidirectionally with training. (*C*) Head volume of sER-free spines decreases with fear conditioning and conditioned inhibition (CI). (*D*) Reconstruction of an SA spine. (*E*) PSD area of SA spines decreases with CI. (*F*) Head volume of SA spines decreases with CI. (*G*) Reconstruction of an sER spine. (*H* and *I*) No change in PSD area (*H*) or head volume (*I*) of sER spines with training. All graphs show means ± SEM (*$P < 0.05$).

Fig. 4. Polyribosomes in spines. (*A*) EM of polyribosomes (arrows) in the dendritic shaft (*Left*) and spine (*Right*). (*B*) Reconstruction of a dendrite with polyribosomes (black) and postsynaptic densities (PSDs) (red). (*C*) There are more polyribosomes in both the dendritic shaft and spines with fear conditioning (FC). (*D*) Polyribosome frequency increases with FC in SA spine heads and smooth endoplasmic reticulum (sER)-free spine bases and necks relative to the naïve group. (*E*) sER-free spines with polyribosomes (+) have smaller PSDs than sER-free spines without polyribosomes (–) in all three training groups. (*F*) SA spines with polyribosomes have larger PSDs than SA spines without polyribosomes in the FC and naïve groups only. SA spines with polyribosomes in the naïve group (+, white bar) have larger PSDs than SA spines with polyribosomes in the conditioned inhibition group (+, gray bar, #*P* < 0.002). (*G*) PSD area on sER spines is unaffected by polyribosomes. All graphs show means ± SEM (**P* < 0.04).

but are instead up-regulated throughout particular dendritic segments; we wondered whether this was related to the presence of particular spine types. In the FC and CI group, shaft polyribosomes correlated with SA spines with polyribosomes, whereas in the naïve group shaft polyribosomes correlated with sER-free spines with polyribosomes (Fig. 5 *B* and *C*). SA spines, although they represent a minority of the spine population, thus appear to be associated with polyribosomes in the shaft after training.

Degradation of soluble proteins via the ubiquitin/proteasome pathway is implicated in hippocampal LTP and destabilization of fear memory (37–39). Whereas we are unable to visualize proteasomes in our material, we can see multivesicular bodies (MVBs), membrane-bound structures containing dense-staining material surrounding a number of clear vesicles (Fig. 5*D*). These organelles occur in dendrites and some spines and are part of the late lysosomal pathway, which degrades membrane-bound proteins (29, 40). We found more MVBs in the dendrites of the FC group (Fig. 5*E*). Their average volume was 0.014 μm^3 and did not change with training (*P* = 0.66). To further examine membrane turnover, we also quantified recycling endosomes in spines. Training did not affect the frequency of spine endosomes, nor was spine endosome frequency correlated with MVB frequency (Fig. S6).

Discussion

It is established that synaptic transmission is enhanced in the LA following fear conditioning, and one report has shown a decrease in synaptic responses to a safety signal (1, 2, 5). There is also evidence that dendritic spines in vitro enlarge or shrink according to the sign of synaptic plasticity (13–16). Although learning-related changes in
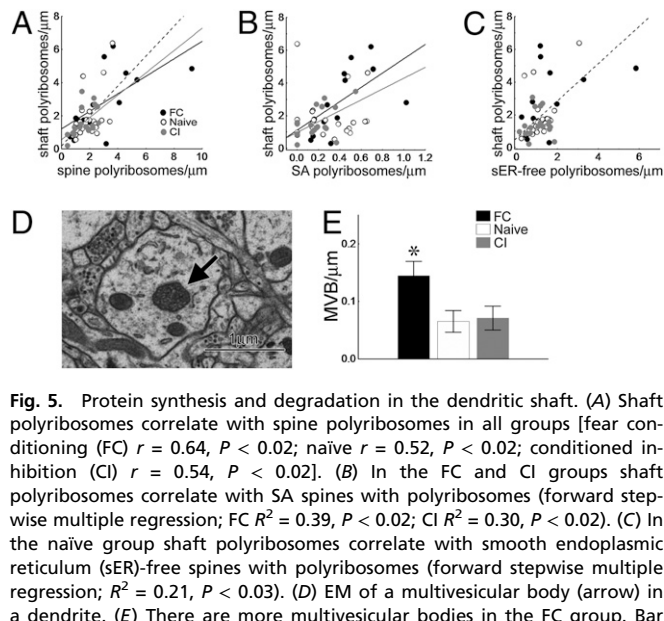
Fig. 5. Protein synthesis and degradation in the dendritic shaft. (*A*) Shaft polyribosomes correlate with spine polyribosomes in all groups [fear conditioning (FC) *r* = 0.64, *P* < 0.02; naïve *r* = 0.52, *P* < 0.02; conditioned inhibition (CI) *r* = 0.54, *P* < 0.02]. (*B*) In the FC and CI groups shaft polyribosomes correlate with SA spines with polyribosomes (forward stepwise multiple regression; FC *R*^{2} = 0.39, *P* < 0.02; CI *R*^{2} = 0.30, *P* < 0.02). (*C*) In the naïve group shaft polyribosomes correlate with smooth endoplasmic reticulum (sER)-free spines with polyribosomes (forward stepwise multiple regression; *R*^{2} = 0.21, *P* < 0.03). (*D*) EM of a multivesicular body (arrow) in a dendrite. (*E*) There are more multivesicular bodies in the FC group. Bar graph shows means ± SEM (**P* < 0.007).

synaptic transmission are hypothesized to involve structural changes at synapses, this has never been explicitly demonstrated. We observed bidirectional changes in LA synapse size corresponding to the value of a fear association, confirming that learning is indeed reflected in synaptic ultrastructure in intact adult animals. We also found that fear and safety learning did not affect spines in the same way and that the differences in the effects of training were related to the spine apparatus, implying a role in memory for this largely neglected organelle.

Although the function of the spine apparatus is unknown, its structure makes it a likely component of stable spines with strong synapses. It is present in the largest spines, which carry the largest, most powerful synapses and have the longest half-life in vivo (10, 41, 42). Its cisterns contain calcium and are continuous with both the sER and the PSD (30, 43, 44), making it well-equipped to mediate calcium signals between the synapse and the dendrite. Its plates contain F-actin and the actin-binding protein synaptopodin, both of which enter and stabilize enlarged spines during hippocampal LTP (45–49). Synaptopodin in dendrites localizes exclusively to the spine apparatus, and spines containing synaptopodin have disproportionally strong synapses for their size, suggesting a role for the spine apparatus beyond simply maintaining large spines (45–49). The addition of the spine apparatus after fear conditioning could thus reflect both an increase in very strong, large synapses and an enhancement in the amount of stable connectivity. Because conditioned inhibition is less robust than fear conditioning, it may simply weaken synapses without destabilizing connections (3, 5).

Fear conditioning increased both polyribosomes and multivesicular bodies in the dendrites, perhaps reflecting a shift in the local protein composition requiring rapid addition of new proteins and removal of old ones. It is unknown whether conditioned inhibition is translation-dependent. Although our results suggest that absolute dendritic translation levels are stable with conditioned inhibition, they do not preclude changes in the identity of the transcripts or in somatic translation. Many dendritic transcripts encode synaptic proteins, suggesting that synaptic maintenance and remodeling could be regulated locally, even at the level of the spine (23, 50). The spine apparatus contains Golgi proteins, which along with the FC-related increase in head polyribosomes suggests that SA spines contain more advanced trans-

NEUROSCIENCE

lation machinery than do sER-free spines (51). SA spine synapses were smaller with conditioned inhibition only when polyribosomes were present. A possible explanation for this is that protein synthesis is initiated by SA spines and is associated with activity. In this scenario, any sufficient activation would produce translation in or even near SA spines, regardless of whether the individual synapse needed new protein. This would explain the presence of shaft polyribosomes in the vicinity of SA spines with both training protocols and would imply a role for the spine apparatus in regulating translation in the local dendrite.

Although we took tissue from an area of LA that receives very heavy auditory inputs to maximize the likelihood of sampling plastic synapses, it is unknown which or what percentage of synapses are activated or altered during learning. We have conducted a population study and our data presumably includes a mixture of synapses that were involved in memory formation and synapses that were not. The relatively small number of spine apparatuses added after fear conditioning and the magnitude of the changes in synapse size likely reflect this fact. A major goal of future work will be to identify altered synapses in a learning paradigm. Memory formation is believed to involve strengthening and stabilization of synapses via new protein synthesis. We have confirmed that synapse structure is altered and local translation is upregulated in the LA during consolidation of fear conditioning. Because fear conditioning memory is essentially permanent and we now know that ultrastructural changes are detectable after learning, this system holds considerable promise for future studies of synaptic memory storage.

Materials and Methods

Subjects and Behavior. Subjects were adult male Sprague-Dawley rats weighing approximately 300 g (Hilltop Lab Animals). Experiments were conducted during the animals' light cycle and all procedures were approved by New York University's Animal Care and Use Committee. Training and testing took place in standard square Coulbourn Instruments and rectangular MED Associates fear conditioning chambers. Scrambled footshocks (1 s, 0.7 mA) were delivered through grid floors and tones (30 s, 80 dB, 5 kHz) were delivered via speakers mounted in the walls (1 per chamber).

Rats were habituated to the Coulbourn chambers for 2 days (30 min/day) before training. The mean intertrial interval (ITI) for tone-shock pairings in the FC protocol was 5 min; in the CI protocol the mean shock-to-tone interval was 119 s and the mean tone-to-shock interval was 180 s. Both protocols lasted a total of 32.5 min. CS-elicited fear was tested with three tone presentations in MED Associates chambers with the grid floors covered by plastic inserts to minimize context generalization. For the context summation test, rats were returned to the Coulbourn chamber and presented with two tones (ITI = 180 s). For the retardation test, rats were given two tone shock pairings (0.4 mA, 1-s shock, ITI = 180 s) in the MED Associates chambers. Memory was tested with five tones in the same chambers with grid floor covers and peppermint soap added to the floor pans.

Tissue Preparation. Rats destined for ssTEM experiments (*n* = 3 per group) were deeply anesthetized with chloral hydrate (1 g/kg i.p.) and perfused transcardially with 50 cc of heparinized saline followed by 500 mL of 2.5% glutaraldehyde/2% paraformaldehyde in 0.1 M phosphate buffer (pH 7.4). Brains were postfixed for 2 h, sectioned at 70 µm on a vibrating slicer (Leica), and the area of tissue around the LA was dissected out. Sections were fixed

in potassium ferrocyanide-reduced osmium (1.5% potassium ferrocyanide/1% osmium in 0.1 M phosphate buffer) followed by 1% osmium tetroxide. Tissue was then dehydrated in a series of ethanols containing 1% uranyl acetate, infiltrated with LX-112 resin (Ladd Research), and cured at 60 °C for 48 h. EM-grade aldehydes, osmium, and uranyl acetate were purchased from Electron Microscopy Sciences.

Serial Sectioning and Electron Microscopy. Serial sections were cut at 45 nm on an Ultracut U microtome (Leica) as described (52). Series ribbons were collected on pioloform-coated single-slot Synaptec grids (Electron Microscopy Sciences) and stained with saturated uranyl acetate and Reynold's lead citrate stain. One series per rat (range 120–160 sections, mean 143) was photographed on a JEOL 1200EX electron microscope at a magnification of 7,500×, and negatives were developed and digitized using a flat bed scanner (Epson).

Serial Reconstruction and Analysis. Digital images were aligned and analyzed using Reconstruct software, and section thickness was estimated from mitochondrial diameters (53, 54). For each series, every spiny dendritic segment that passed through the central section and was complete and in cross-section within the tissue volume was reconstructed with the experimenters blind to training group. We used diameter and microtubule number to confirm that we sampled a homogenous population across series; these were correlated and did not differ between training groups (Fig. S7). For frequency measurements, dendritic length was measured from the origin of the first protrusion on an arbitrarily chosen inclusion end to the origin of the last spine on the other end, with the final protrusion excluded from the count. Approximately 9% of protrusion origins in all groups gave rise to multiple branches; these did not differ from single branches in any of our measures and were thus counted as individual protrusions. The dataset included 69 dendritic segments (average length = 6.5 µm) with 1,037 protrusions, 1,021 spine synapses, and 216 shaft synapses; 1,475 polyribosomes, 56 multivesicular bodies, and 464 spine surface areas were included. The micrographs from one series did not consistently have sufficient resolution for identification of polyribosomes, so it was excluded from that analysis. Images of 3D reconstructions were rendered in 3DS Max software (Autodesk).

Statistics. For behavior data, group means of freezing scores were compared across animals by ANOVA followed by Tukey's post hoc test. For within-animal behavior comparisons paired, two-tailed *t* tests were used. For comparisons of spine and dendrite measurements between training groups, hierarchical ANOVAs were used with rats nested into training procedure, followed by the Fisher LSD test. For effects of training, p values are only reported for significant differences between the naïve group and the FC or CI group. In instances where it is stated that a measure was not changed between training groups or for analyses in which multiple groups were collapsed, a factorial ANOVA was used to ensure that there were no significant interactions between groups and independent variables. In these cases rat was always included as a factor to verify that there was no interaction. Except where stated otherwise, correlations are simple regression and were always run on each training group independently; r^2 is reported for $P < 0.05$. PSD areas, spine volumes, and spine surface areas were subjected to a logarithmic transformation for ANOVA.

1. Sah P, Westbrook RF, Lüthi A (2008) Fear conditioning and long-term potentiation in the amygdala: What really is the connection? *Ann N Y Acad Sci* 1129:88–95.
2. LeDoux JE (2000) Emotion circuits in the brain. *Annu Rev Neurosci* 23:155–184.
3. Rescorla RA (1969) Conditioned inhibition of fear resulting from negative CS-US contingencies. *J Comp Physiol Psychol* 67:504–509.
4. Rogan MT, Stäubli UV, LeDoux JE (1997) Fear conditioning induces associative long-term potentiation in the amygdala. *Nature* 390:604–607.
5. Rogan MT, Leon KS, Perez DL, Kandel ER (2005) Distinct neural signatures for safety and danger in the amygdala and striatum of the mouse. *Neuron* 46:309–320.
6. Sigurdsson T, Doyère V, Cain CK, LeDoux JE (2007) Long-term potentiation in the amygdala: A cellular mechanism of fear learning and memory. *Neuropharmacology* 52:215–227.
7. Farb CR, LeDoux JE (1997) NMDA and AMPA receptors in the lateral nucleus of the amygdala are postsynaptic to auditory thalamic afferents. *Synapse* 27:106–121.
8. Farb CR, Ledoux JE (1999) Afferents from rat temporal cortex synapse on lateral amygdala neurons that express NMDA and AMPA receptors. *Synapse* 33:218–229.
9. Bourne JN, Harris KM (2008) Balancing structure and function at hippocampal dendritic spines. *Annu Rev Neurosci* 31:47–67.
10. Kasai H, Matsuzaki M, Noguchi J, Yasumatsu N, Nakahara H (2003) Structure-stability-function relationships of dendritic spines. *Trends Neurosci* 26:360–368.
11. Yuste R, Bonhoeffer T (2001) Morphological changes in dendritic spines associated with long-term synaptic plasticity. *Annu Rev Neurosci* 24:1071–1089.
12. Humeau Y, et al. (2005) Dendritic spine heterogeneity determines afferent-specific Hebbian plasticity in the amygdala. *Neuron* 45:119–131.
13. Matsuzaki M, Honkura N, Ellis-Davies GC, Kasai H (2004) Structural basis of long-term potentiation in single dendritic spines. *Nature* 429:761–766.
14. Zhou Q, Homma KJ, Poo MM (2004) Shrinkage of dendritic spines associated with long-term depression of hippocampal synapses. *Neuron* 44:749–757.

15. Wang XB, Yang Y, Zhou Q (2007) Independent expression of synaptic and morphological plasticity associated with long-term depression. *J Neurosci* 27:12419–12429.
16. Tanaka J, et al. (2008) Protein synthesis and neurotrophin-dependent structural plasticity of single dendritic spines. *Science* 319:1683–1687.
17. Bourne J, Harris KM (2007) Do thin spines learn to be mushroom spines that remember? *Curr Opin Neurobiol* 17:381–386.
18. Jedlicka P, Vlachos A, Schwarzacher SW, Deller T (2008) A role for the spine apparatus in LTP and spatial learning. *Behav Brain Res* 192:12–19.
19. Huang YY, Martin KC, Kandel ER (2000) Both protein kinase A and mitogen-activated protein kinase are required in the amygdala for the macromolecular synthesis-dependent late phase of long-term potentiation. *J Neurosci* 20:6317–6325.
20. Schafe GE, LeDoux JE (2000) Memory consolidation of auditory Pavlovian fear conditioning requires protein synthesis and protein kinase A in the amygdala. *J Neurosci* 20:96RC.
21. Maren S, Ferrario CR, Corcoran KA, Desmond TJ, Frey KA (2003) Protein synthesis in the amygdala, but not the auditory thalamus, is required for consolidation of Pavlovian fear conditioning in rats. *Eur J Neurosci* 18:3080–3088.
22. Frey U, Krug M, Brödemann R, Reymann K, Matthies H (1989) Long-term potentiation induced in dendrites separated from rat's CA1 pyramidal somata does not establish a late phase. *Neurosci Lett* 97:135–139.
23. Sutton MA, Schuman EM (2006) Dendritic protein synthesis, synaptic plasticity, and memory. *Cell* 127:49–58.
24. Martin KC, Zukin RS (2006) RNA trafficking and local protein synthesis in dendrites: An overview. *J Neurosci* 26:7131–7134.
25. Helmstetter FJ, Parsons RG, Gafford GM (2008) Macromolecular synthesis, distributed synaptic plasticity, and fear conditioning. *Neurobiol Learn Mem* 89:324–337.
26. McDonald AJ (1998) Cortical pathways to the mammalian amygdala. *Prog Neurobiol* 55:257–332.
27. Shi CJ, Cassell MD (1997) Cortical, thalamic, and amygdaloid projections of rat temporal cortex. *J Comp Neurol* 382:153–175.
28. Gray EG (1959) Axo-somatic and axo-dendritic synapses of the cerebral cortex: An electron microscope study. *J Anat* 93:420–433.
29. Spacek J, Harris KM (1997) Three-dimensional organization of smooth endoplasmic reticulum in hippocampal CA1 dendrites and dendritic spines of the immature and mature rat. *J Neurosci* 17:190–203.
30. Tarrant SB, Routtenberg A (1979) Postsynaptic membrane and spine apparatus: Proximity in dendritic spines. *Neurosci Lett* 11:289–294.
31. Harris KM, Stevens JK (1988) Dendritic spines of rat cerebellar Purkinje cells: Serial electron microscopy with reference to their biophysical characteristics. *J Neurosci* 8:4455–4469.
32. Harris KM, Stevens JK (1989) Dendritic spines of CA 1 pyramidal cells in the rat hippocampus: Serial electron microscopy with reference to their biophysical characteristics. *J Neurosci* 9:2982–2997.
33. Knott GW, Holtmaat A, Wilbrecht L, Welker E, Svoboda K (2006) Spine growth precedes synapse formation in the adult neocortex in vivo. *Nat Neurosci* 9:1117–1124.
34. Steward O, Levy WB (1982) Preferential localization of polyribosomes under the base of dendritic spines in granule cells of the dentate gyrus. *J Neurosci* 2:284–291.
35. Ostroff LE, Fiala JC, Allwardt B, Harris KM (2002) Polyribosomes redistribute from dendritic shafts into spines with enlarged synapses during LTP in developing rat hippocampal slices. *Neuron* 35:535–545.
36. Bourne JN, Sorra KE, Hurlburt J, Harris KM (2007) Polyribosomes are increased in spines of CA1 dendrites 2 h after the induction of LTP in mature rat hippocampal slices. *Hippocampus* 17:1–4.
37. Karpova A, Mikhaylova M, Thomas U, Knöpfel T, Behnisch T (2006) Involvement of protein synthesis and degradation in long-term potentiation of Schaffer collateral CA1 synapses. *J Neurosci* 26:4949–4955.
38. Fonseca R, Vabulas RM, Hartl FU, Bonhoeffer T, Nägerl UV (2006) A balance of protein synthesis and proteasome-dependent degradation determines the maintenance of LTP. *Neuron* 52:239–245.
39. Lee SH, et al. (2008) Synaptic protein degradation underlies destabilization of retrieved fear memory. *Science* 319:1253–1256.
40. Katzmann DJ, Odorizzi G, Emr SD (2002) Receptor downregulation and multivesicular-body sorting. *Nat Rev Mol Cell Biol* 3:893–905.
41. Holtmaat A, Wilbrecht L, Knott GW, Welker E, Svoboda K (2006) Experience-dependent and cell-type-specific spine growth in the neocortex. *Nature* 441:979–983.
42. Matsuzaki M, et al. (2001) Dendritic spine geometry is critical for AMPA receptor expression in hippocampal CA1 pyramidal neurons. *Nat Neurosci* 4:1086–1092.
43. Spacek J (1985) Three-dimensional analysis of dendritic spines. II. Spine apparatus and other cytoplasmic components. *Anat Embryol (Berl)* 171:235–243.
44. Fifková E, Markham JA, Delay RJ (1983) Calcium in the spine apparatus of dendritic spines in the dentate molecular layer. *Brain Res* 266:163–168.
45. Deller T, Merten T, Roth SU, Mundel P, Frotscher M (2000) Actin-associated protein synaptopodin in the rat hippocampal formation: Localization in the spine neck and close association with the spine apparatus of principal neurons. *J Comp Neurol* 418:164–181.
46. Capani F, Martone ME, Deerinck TJ, Ellisman MH (2001) Selective localization of high concentrations of F-actin in subpopulations of dendritic spines in rat central nervous system: A three-dimensional electron microscopic study. *J Comp Neurol* 435:156–170.
47. Fukazawa Y, et al. (2003) Hippocampal LTP is accompanied by enhanced F-actin content within the dendritic spine that is essential for late LTP maintenance in vivo. *Neuron* 38:447–460.
48. Honkura N, Matsuzaki M, Noguchi J, Ellis-Davies GC, Kasai H (2008) The subspine organization of actin fibers regulates the structure and plasticity of dendritic spines. *Neuron* 57:719–729.
49. Vlachos A, et al. (2009) Synaptopodin regulates plasticity of dendritic spines in hippocampal neurons. *J Neurosci* 29:1017–1033.
50. Kelleher RJ, 3rd, Govindarajan A, Tonegawa S (2004) Translational regulatory mechanisms in persistent forms of synaptic plasticity. *Neuron* 44:59–73.
51. Pierce JP, Mayer T, McCarthy JB (2001) Evidence for a satellite secretory pathway in neuronal dendritic spines. *Curr Biol* 11:351–355.
52. Harris KM, et al. (2006) Uniform serial sectioning for transmission electron microscopy. *J Neurosci* 26:12101–12103.
53. Fiala JC (2005) Reconstruct: A free editor for serial section microscopy. *J Microsc* 218:52–61.
54. Fiala JC, Harris KM (2001) Cylindrical diameters method for calibrating section thickness in serial electron microscopy. *J Microsc* 202:468–472.

NEUROSCIENCE